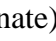


## LIST OF FIGURES

Figure	Page No.
<b>1.1</b> Structural classification of metal-dioxygen complexes (L = Ligand).	1.5
<b>1.2</b> The structure of the $[\text{Nb}(\text{O}_2)_4]^{3-}$ anion in $\text{Na}_3[\text{Nb}(\text{O}_2)_4] \cdot 13\text{H}_2\text{O}$ showing the disorder in the peroxo oxygen atom positions. Two different conformations are shown in black and white lines.	1.7
<b>1.3</b> Environment of the metal atom reported for halide-free homometallic heteroleptic peroxo complexes of niobium derived from the corresponding tetraperoxoniobate.	1.11
<b>1.4</b> Structure and atom numbering of $[\text{Nb}(\text{O}_2)_3(\text{quin-2-c})]^{2-}$ . Thermal ellipsoids are drawn at the 50% probability level.	1.12
<b>1.5</b> ORTEP plot of the molecular anion, $[\text{Nb}_2(\text{O}_2)_4(\text{tart})(\text{Htart})]^{5-}$ (50% probability).	1.13
<b>1.6</b> The peroxoniobium complexes tested for (A) insulin-like activity: $[\text{Nb}(\text{O}_2)_4]^{3-}$ and $[\text{Nb}(\text{O}_2)_3(\text{quin-2-c})]^{2-}$ and (B) anti-cancer activity: $[\text{Nb}(\text{Asc})(\text{O}_2)_3]^{3-}$ .	1.14
<b>1.7</b> Selected oxidations of organic compounds by Nb-peroxo systems in the presence of hydrogen peroxide.	1.17
<b>1.8</b> Type I: Metal ions, complexes, chelates at macromolecules.	1.22
<b>1.9</b> (A) Type II: Ligand of metal complexes, chelates as part of linear or crosslinked macromolecules. (B) Type III: Metal as part of a linear chain or network. (C) Type IV: Physical incorporation of metal complexes, chelates.	1.23
<b>1.10</b> Some water-soluble polymer used for metal ion interaction.	1.26
<b>1.11</b> “Metallic-arrows” tailored with targeting vectors which will efficiently shot to the cancer cells.	1.30
<b>3.1</b> Scanning electron micrographs of (a) PA, (b) <b>PANb (3.1)</b> and (c) PSS, (d) <b>PSSNb (3.2)</b> .	3.8
<b>3.2</b> EDX spectra of (a) <b>PANb (3.1)</b> and (b) <b>PSSNb (3.2)</b> .	3.8
<b>3.3</b> IR spectra of (a) PA and (b) <b>PANb</b> .	3.12
<b>3.4</b> (a) IR & (b) Raman spectra of <b>PANb</b> .	3.12
<b>3.5</b> IR spectra of (a) PSS and (b) <b>PSSNb</b> .	3.13

<b>3.6</b>	(a) IR & (b) Raman spectra of <b>PSSNb</b> .	3.13
<b>3.7</b>	TGA-DTG plots of <b>PANb</b> .	3.15
<b>3.8</b>	TGA-DTG plot of <b>PSSNb</b> .	3.15
<b>3.9</b>	<sup>13</sup> C NMR spectra of (a) PA and (b) <b>PANb</b> in D <sub>2</sub> O.	3.17
<b>3.10</b>	<sup>13</sup> C NMR spectra of (a) PSS and (b) <b>PSSNb</b> in D <sub>2</sub> O.	3.17
<b>3.11</b>	<sup>93</sup> Nb NMR spectra of 0.2 mM solution of (a) <b>NaNb</b> , (b) <b>PANb</b> and (c) <b>PSSNb</b> in D <sub>2</sub> O.	3.19
<b>3.12</b>	Proposed structures of soluble polymer anchored pNb complexes, (A) <b>PANb</b> (3.1) and (B) <b>PSSNb</b> (3.2). PA = poly(sodium acrylate), PSS = poly(sodium styrene sulfonate) and “  ” represents polymer chain.	3.20
<b>3.13</b>	Optimized geometry of <b>PANb</b> complex obtained by using density functional theory (DFT). The numerical numbers represent the labeling of the atoms as in <b>Table 3.4</b> . (Colors: light blue is niobium, red is oxygen, grey is carbon and dark blue lines represent hydrogen).	3.22
<b>3.14</b>	Optimized geometry of <b>PSSNb</b> complex obtained by using density functional theory (DFT). The numerical numbers represent the labeling of the atoms as in <b>Table 3.4</b> . (Colors: light blue is niobium, red is oxygen, yellow is sulfur, grey is carbon, dark blue is hydrogen and purple lines represent sodium).	3.22
<b>3A.1</b>	Raman spectrum of <b>PANb</b> .	3.25
<b>3A.2</b>	IR spectrum of the residue after TGA of <b>PANb</b> up to 700 °C.	3.25
<b>4.1</b>	A view of the asymmetric unit of [Cu(arg) <sub>2</sub> (H <sub>2</sub> O)]NaNO <sub>3</sub> , showing displacement ellipsoids drawn at the 30% probability level.	4.3
<b>4.2</b>	IR spectrum of <b>KNb</b> .	4.9
<b>4.3</b>	IR spectra of (a) alanine and (b) <b>NbAla</b> .	4.11
<b>4.4</b>	(a) IR & (b) Raman spectra of <b>NbAla</b> .	4.11
<b>4.5</b>	IR spectra of (a) valine and (b) <b>NbVal</b> .	4.12
<b>4.6</b>	(a) IR & (b) Raman spectra of <b>NbVal</b> .	4.12
<b>4.7</b>	IR spectra of (a) arginine and (b) <b>NbA</b> .	4.13
<b>4.8</b>	(a) IR & (b) Raman spectra of <b>NbA</b> .	4.13
<b>4.9</b>	IR spectra of (a) nicotinic acid and (b) <b>NbN</b> .	4.15
<b>4.10</b>	(a) IR & (b) Raman spectra of <b>NbN</b> .	4.15

4.11	<sup>1</sup> H NMR spectrum of <b>NbAla</b> in D <sub>2</sub> O.	4.18
4.12	<sup>1</sup> H NMR spectrum of <b>NbVal</b> in D <sub>2</sub> O.	4.18
4.13	<sup>1</sup> H NMR spectrum of <b>NbA</b> in D <sub>2</sub> O.	4.19
4.14	<sup>1</sup> H NMR spectrum of <b>NbN</b> in D <sub>2</sub> O.	4.19
4.15	<sup>13</sup> C NMR spectra of (a) alanine and (b) <b>NbAla</b> in D <sub>2</sub> O.	4.22
4.16	<sup>13</sup> C NMR spectra of (a) valine and (b) <b>NbVal</b> in D <sub>2</sub> O.	4.22
4.17	<sup>13</sup> C NMR spectra of (a) arginine and (b) <b>NbA</b> in D <sub>2</sub> O.	4.23
4.18	<sup>13</sup> C NMR spectra of (a) nicotinic acid and (b) <b>NbN</b> in D <sub>2</sub> O.	4.23
4.19	<sup>93</sup> Nb NMR spectra of (a) <b>KNb</b> , (b) <b>NbAla (4.1)</b> , (c) <b>NbVal (4.2)</b> , (d) <b>NbA (4.3)</b> and (e) <b>NbN (4.4)</b> in D <sub>2</sub> O.	4.24
4.20	TGA-DTG plot of <b>KNb</b>	4.25
4.21	TGA-DTG plot of <b>NbAla</b> .	4.27
4.22	TGA-DTG plot of <b>NbVal</b> .	4.27
4.23	TGA-DTG plot of <b>NbA</b> .	4.28
4.24	TGA-DTG plot of <b>NbN</b> .	4.28
4.25	Proposed structure of (a) <b>NbAla (4.1)</b> , (b) <b>NbVal (4.2)</b> , (c) <b>NbA (4.3)</b> and (d) <b>NbN (4.4)</b> .	4.30
4.26	Optimized geometry of (a) <b>NbAla (4.1)</b> , (b) <b>NbVal (4.2)</b> , (c) <b>NbA (4.3)</b> and (d) <b>NbN (4.4)</b> . The numerical numbers represent the labeling of the atoms as in <b>Table 4.6</b> .	4.31
4.27	ORTEP of <b>KNb</b> with 50% probability ellipsoid [asymmetric unit].	4.33
5.1	Catalyst regeneration up to 6 <sup>th</sup> reaction cycle. Recyclability of <b>NbA</b> (used as representative catalyst) for the selective oxidation of MPS to (a) sulfoxide or (b) sulfone.	5.21
5.2	Catalyst regeneration up to 6 <sup>th</sup> reaction cycle. Recyclability of <b>PSSNb</b> (used as representative catalyst for macro pNb complex) for the selective oxidation of MPS to (a) sulfoxide or (b) sulfone.	5.21
5.3	IR spectra of (a) <b>NbA</b> , (b) Regenerated <b>NbA</b> after the 2 <sup>nd</sup> cycle of reaction and (c) Diperoxoniobate complex recovered after oxidation of MPS by <b>NbA</b> , in absence of H <sub>2</sub> O <sub>2</sub> .	5.22
5.4	Schematic representation of reactions occurring with pNb catalysts, <b>NbA (4.3)</b> as representative.	5.24
5A.1	<sup>1</sup> H NMR spectra of methyl phenyl sulfoxide.	5.25

<b>5A.2</b>	<sup>13</sup> C NMR spectra of methyl phenyl sulfoxide.	5.25
<b>5A.3</b>	<sup>1</sup> H NMR spectra of methyl phenyl sulfone.	5.26
<b>5A.4</b>	<sup>13</sup> C NMR spectra of methyl phenyl sulfone.	5.26
<b>6.1</b>	The <sup>1</sup> H NMR spectra of <b>NbA</b> in D <sub>2</sub> O. The spectra were recorded as follows: (a) <b>NbA</b> in D <sub>2</sub> O immediately after preparation, (b) solution of (a) 12 h later.	6.5
<b>6.2</b>	The <sup>13</sup> C NMR spectra of <b>NbA</b> in D <sub>2</sub> O. The spectra were recorded as follows: (a) <b>NbA</b> in D <sub>2</sub> O immediately after preparation, (b) solution of (a) 12 h later.	6.6
<b>6.3</b>	Stability of compound <b>NaNb</b> at different pH values: (▲) compound solution in distilled water, pH of the solution = 10.0, (X) solution of complexes in phosphate buffer (50 mM, pH 7.0). Stability of compound <b>NbA</b> (3.3) at different pH values: (■) compound solution in distilled water, pH of the solution = 9.0, (⌘) solution of complexes in phosphate buffer (50 mM, pH 7.0). Effect of catalase on (x) <b>NaNb</b> , (▲) <b>KNb</b> , (◆) <b>PANb</b> (3.1), (■) <b>PSSNb</b> (3.2), (+) <b>NbAla</b> (4.1), (-) <b>NbVal</b> (4.2), (⌘) <b>NbA</b> (4.3) and (●) <b>NbN</b> (4.4).	6.7
<b>6.4</b>	Effect of catalase on (a) <b>NaNb</b> , (b) <b>NbVal</b> (4.2), (c) <b>NbA</b> (4.3) and (d) <b>NbN</b> (4.4). The test solution contained (◆) phosphate buffer or (■) HEPES buffer (50 mM, pH 7.0) and the catalase (40 µg/mL) which was incubated at 30 °C for 5 min.	6.10
<b>6.5</b>	<sup>93</sup> Nb NMR spectra of a 0.2 mM solution of <b>PANb</b> , its catalase degradation products. The spectra were recorded as follows: (a) aqueous solution of <b>PANb</b> in water immediately after preparation, (b) <b>PANb</b> (20 mM) incubated with catalase (40 mg/mL) after 30 min incubation, (c) solution of (b) 1 h later and (d) solution of (b) 2 h later.	6.11
<b>6.6</b>	The viability of Raw 264.7 murine macrophage cells as measured by the MTT assay. Cells were treated with the monomeric pNb compounds ( <b>NaNb</b> and <b>4.1-4.4</b> ) and incubated for 24 h. MTT was added to the cells and incubated for 4 h. The cell viability was assessed by measuring the absorbance at 580 nm and expressed as mean (± SE) from three separate experiments.	6.12

<b>6A.1</b>	The $^1\text{H}$ NMR spectra of <b>NbAla</b> in $\text{D}_2\text{O}$ . The spectra were recorded as follows: (a) <b>NbAla</b> in $\text{D}_2\text{O}$ immediately after preparation, (b) solution of (a) 12 h later.	6.14
<b>6A.2</b>	The $^{13}\text{C}$ NMR spectra of <b>NbAla</b> in $\text{D}_2\text{O}$ . The spectra were recorded as follows: (a) <b>NbAla</b> in $\text{D}_2\text{O}$ immediately after preparation, (b) solution of (a) 12 h later.	6.14
<b>6A.3</b>	The $^1\text{H}$ NMR spectra of <b>NbVal</b> in $\text{D}_2\text{O}$ . The spectra were recorded as follows: (a) <b>NbVal</b> in $\text{D}_2\text{O}$ immediately after preparation, (b) solution of (a) 12 h later.	6.15
<b>6A.4</b>	The $^{13}\text{C}$ NMR spectra of <b>NbVal</b> in $\text{D}_2\text{O}$ . The spectra were recorded as follows: (a) <b>NbVal</b> in $\text{D}_2\text{O}$ immediately after preparation, (b) solution of (a) 12 h later.	6.15
<b>6A.5</b>	The $^1\text{H}$ NMR spectra of <b>NbN</b> in $\text{D}_2\text{O}$ . The spectra were recorded as follows: (a) <b>NbN</b> in $\text{D}_2\text{O}$ immediately after preparation, (b) solution of (a) 12 h later.	6.16
<b>6A.6</b>	The $^{13}\text{C}$ NMR spectra of <b>NbN</b> in $\text{D}_2\text{O}$ . The spectra were recorded as follows: (a) <b>NbN</b> in $\text{D}_2\text{O}$ immediately after preparation, (b) solution of (a) 12 h later.	6.16
<b>6A.7</b>	The $^{13}\text{C}$ NMR spectra of <b>PANb</b> in $\text{D}_2\text{O}$ . The spectra were recorded as follows: (a) <b>PANb</b> in $\text{D}_2\text{O}$ immediately after preparation, (b) solution of (a) 12 h later.	6.17
<b>6A.8</b>	The $^{13}\text{C}$ NMR spectra of <b>PSSNb</b> in $\text{D}_2\text{O}$ . The spectra were recorded as follows: (a) <b>PSSNb</b> in $\text{D}_2\text{O}$ immediately after preparation, (b) solution of (a) 12 h later.	6.17
<b>7.1</b>	General structures of plant (A) and animal (B) PAPs. Most of the plant PAPs reported to date are homodimeric with 55 kDa subunits whereas the animal PAPs studied to date are 35 kDa monomers. Each subunit has two domains viz., an N-terminal domain without known function and a C-terminal domain that contains the active site.	7.3
<b>7.2</b>	Schematic of the active site of kidney bean purple acid phosphatase based on the 2.65-Å resolution structure described by Klabunde <i>et al.</i>	7.4
<b>7.3</b>	The effect of synthesized pNb compounds and free ligand on the activity of ACP.	7.7

<b>7.4</b>	Lineweaver-Burk plots for the inhibition of ACP activity in the absence and presence of (A) <b>NaNb</b> , (B) <b>KNb</b> , (C) <b>NbAla</b> and (D) <b>NbVal</b> . The inset represents the secondary plot of the initial kinetic data of the Lineweaver-Burk plot.	7.9
<b>7.5</b>	Lineweaver-Burk plots for the inhibition of ACP activity in the absence and presence of (A) <b>NbA</b> , (B) <b>NbN</b> (C) <b>PANb</b> and (D) <b>PSSNb</b> . The inset represents the secondary plot of the initial kinetic data of the Lineweaver-Burk plot.	7.10
<b>8.1</b>	The structure of $\text{Ca}^{2+}/\text{CaM-CN}$ complex.	8.3
<b>8.2</b>	Schematic of the active site of human calcineurin based on the 2.1-Å resolution structure described by Kissinger <i>et al.</i>	8.3
<b>8.3</b>	Inhibitors of calcineurin (a) cyclosporine A (CsA) and (b) FK506 (tactolimus).	8.4
<b>8.4</b>	The effect of pNb compounds and $\text{H}_2\text{O}_2$ on calcineurin activity, (a) effect of <b>NaNb</b> and <b>PANb (3.1)</b> on calcineurin activity with RII-phosphopeptide as substrate, (b) effect of <b>NaNb</b> and <b>PANb (3.1)</b> on calcineurin activity with p-NPP as substrate and (c) effect of $\text{H}_2\text{O}_2$ on calcineurin activity.	8.8
<b>8.5</b>	Lineweaver-Burk plots for inhibition of calcineurin activity in absence and presence of (A) <b>NaNb</b> , (B) <b>PANb (3.1)</b> and (C) $\text{H}_2\text{O}_2$ . The inset represents the secondary plot of the initial kinetic data of the Lineweaver-Burk plot.	8.10

---

## LIST OF SCHEMES

Scheme		Page No.
1.1	pH-dependence of the substitution of fluoro ligands by peroxy groups in niobate complexes.	1.7
1.2	An illustration of the green synthetic approach for preparation of KNN powders from aqueous solutions through (a) niobium(V)-peroxy-citrate (b) niobium(V)-peroxy-glycine precursors.	1.15
1.3	Plausible mechanism for the epoxidation using pre-treated Nb(salan)(OiPr) <sub>3</sub> as a catalyst.	1.19
1.4	Proposed mechanism for epoxidation of allylic alcohols with H <sub>2</sub> O <sub>2</sub> catalyzed by the monomeric peroxyoniobate anion of IL.	1.20

## LIST OF TABLES

Table	Page No.
<b>1.1</b> Some homoleptic and heteroleptic peroxoniobate (pNb) complexes described in the literature	1.9 & 1.10
<b>1.2</b> The summary of combinations of metal complexes and macroligands, as well as catalyzed reactions most commonly used in practice	1.24
<b>3.1</b> Analytical data for the polymer-bound peroxoniobate compounds	3.9
<b>3.2</b> Experimental and theoretical infrared and Raman spectral data (cm <sup>-1</sup> ) for <b>PANb (3.1)</b> and <b>PSSNb (3.2)</b>	3.11
<b>3.3</b> <sup>13</sup> C NMR spectral data for <b>PANb</b> and <b>PSSNb</b>	3.18
<b>3.4</b> Selected bond lengths (Å) and bond angles (degree) for <b>PANb</b> and <b>PSSNb</b> complexes calculated using density functional theory (DFT) as implemented in the DMol <sup>3</sup> package	3.23
<b>4.1</b> Analytical data for the synthesized peroxy-niobium complexes	4.8
<b>4.2</b> Experimental and theoretical infrared and Raman spectral data (in cm <sup>-1</sup> ) for the compounds, <b>NbAla</b> , <b>NbVal</b> , <b>NbA</b> and <b>NbN</b>	4.16
<b>4.3</b> <sup>1</sup> H NMR chemical shifts for ligands and heteroligand peroxy-niobate complexes	4.20
<b>4.4</b> <sup>13</sup> C NMR chemical shift for ligands and the developed triperoxoniobium complexes	4.21
<b>4.5</b> Thermogravimetric data of peroxoniobium compounds, <b>KNb</b> and <b>4.1-4.4</b>	4.29
<b>4.6</b> Selected bond lengths (in Å) and bond angles (in degree) for the pNb complexes calculated at B3LYP/LANL2DZ level of theory	4.32
<b>4.7</b> Crystallographic data of K <sub>3</sub> [Nb(O <sub>2</sub> ) <sub>4</sub> ] ( <b>KNb</b> ), compared with reported Sodium tetraperoxoniobate Na <sub>3</sub> [Nb(O <sub>2</sub> ) <sub>4</sub> ]·13H <sub>2</sub> O ( <b>NaNb</b> )	4.34
<b>4.8</b> Description of crystal data	4.35 & 4.36
<b>5.1</b> Optimization of reaction conditions for selective oxidation of methyl phenyl sulfide (MPS) by 30% H <sub>2</sub> O <sub>2</sub> catalyzed by pNb complexes	5.8



<b>5.2</b>	Selective oxidation of sulfides to sulfoxides catalyzed by <b>NbA</b> and <b>NbN</b>	5.10
<b>5.3</b>	Selective oxidation of sulfides to sulfoxides catalyzed by <b>PANb</b> and <b>PSSNb</b>	5.12
<b>5.4</b>	Optimization of reaction conditions for <b>NbA</b> catalyzed selective oxidation of methyl phenyl sulfide (MPS) to sulfone	5.15
<b>5.5</b>	Selective oxidation of sulfides to sulfones catalyzed by <b>NbA</b> and <b>NbN</b>	5.16
<b>5.6</b>	Selective oxidation of sulfides to sulfones catalyzed by <b>PANb</b> and <b>PSSNb</b>	5.18
<b>6.1</b>	Catalase-dependent oxygen release from niobiumperoxo compounds	6.8
<b>6.2</b>	Effect on Raw 264.7 murine macrophage cells when treated with peroxoniobium complexes at 200 $\mu$ M concentration of pNb compounds	6.12
<b>7.1</b>	Half-maximal inhibitory concentration ( $IC_{50}$ ) and inhibitor constants ( $K_i$ and $K_{ii}$ ) values for pNb compounds	7.11
<b>8.1</b>	Half-maximal inhibitory concentration ( $IC_{50}$ ) and inhibitor constant ( $K_{iu}$ ) values for pNb compounds and $H_2O_2$ against calcineurin	8.11

---

## LIST OF ABBREVIATIONS

ACP	acid phosphatase
ALP	alkaline phosphatase
CTS	chitosan
Cp	cyclopentadienyl
DBT	dibenzothiophene
DMF	dimethyl formamide
dipy	dipyridyl
CSDVB	cross-linked poly(styrene-divinyl benzene)
DFT	density functional theory
DNA	deoxyribonucleic acid
DSSCs	dye sensitized solar cells
DTG	differential thermogravimetry
EDTA	ethylenediaminetetraacetic acid
EDX	energy dispersive X-Ray analysis
GC	gas chromatography
gu	guanidinium
HEPES	4-(2-hydroxyethyl)-1-piperazineethanesulfonic acid
H <sub>2</sub> salen	bis(salicylaldehyde)ethylenediamine
H <sub>2</sub> hned	bis(2-hydroxy-1-naphthaldehyde)ethylenediamine
H <sub>2</sub> acen	bis(acetylacetonate)ethylenediamine
H <sub>2</sub> salphen	bis(salicylaldehyde)phenylenediamine
H <sub>2</sub> anac	acetylacetonatebis(anthranilic acid)
H <sub>2</sub> salpren	bis(salicylaldehyde)propylenediamine
H <sub>2</sub> sap	salicylaldehyde o-aminophenol
H <sub>2</sub> hntrien	bis(2-hydroxy-1-naphthaldehyde)1,2-aminopropane
H <sub>3</sub> mal	malic acid
H <sub>4</sub> edta	ethylenediaminetetraacetic acid
H <sub>4</sub> pda	propylenediaminetetraacetic acid
H <sub>5</sub> dtpa	diethylenetriaminepentaacetic acid
H <sub>6</sub> ttha	triethylenetetraaminehexaacetic acid
H <sub>2</sub> dipic	dipicolinic acid

H4tart	tartaric acid
H2ox	oxalic acid
H4cit	citric acid
H2glyc	glycolic acid
HIV	human immunodeficiency virus
HPLC	high Performance Liquid Chromatography
hq	8-quinolinolate
IC <sub>50</sub>	half-maximal inhibitory concentration
IR	infra red
KNb	$K_3[Nb(O_2)_4]$
LD <sub>50</sub>	Lethal Dose, 50%
MPS	methyl phenyl sulfide
MR	Merrifield resin
NaNb	$Na_3[Nb(O_2)_4] \cdot 13H_2O$
NbA	$Na_2[Nb(O_2)_3(arg)] \cdot 2H_2O$
NbAla	$Na_2[Nb(O_2)_3alaninato]$
NbN	$Na_2[Nb(O_2)_3(nic)(H_2O)] \cdot H_2O$
NbVal	$Na_2[Nb(O_2)_3 valinato]$
NMR	nuclear magnetic resonance
PA	poly(sodium acrylate)
PAA	polyacrylic acid
PAC	polyaminocarboxylate
PAm	poly(acryl amide)
PAN	poly(acrylonitrile)
PANb	$[Nb_2(O_2)_6(carboxylate)_2]-PA$
PAV	$Na_3[V_2O_2(O_2)_4(carboxylate)]-PA$
PEG	poly(ethylene glycol)
PEI	polyethyleneimine
PEO	poly(ethylene oxide)
phen	1,10-phenantroline
pic <sup>-</sup>	picolinato
picO <sup>-</sup>	picolinato N-oxide
PMA	sodium polymethacrylate
PMAA	poly(methacrylamide)

PMMA	poly(methylmethacrylate)
pMo	peroxomolybdate
pNb	peroxoniobate
PS	poly(styrene)
PSNa	poly(sodium vinyl sulfonate)
PSS	poly(sodium 4-styrene sulfonate)
PSSNb	[Nb(O <sub>2</sub> ) <sub>3</sub> (sulfonate) <sub>2</sub> ]-PSS
p-NPP	p-nitrophenyl phosphate
p-NP	p-nitrophenol
PTC	phase transfer catalyst
pzdc	pyrazine 2,5-dicarboxylate
pV	peroxovanadate
PVA	polyvinyl alcohol
pW	peroxotungstate
PTPase	phosphotyrosine phosphatase
quin-2-c	quinoline-2-carboxylate ion
RT	room temperature
RNA	ribonucleic acid
SEM	scanning electron microscopy
TGA	thermogravimetry analysis
TLC	thin layer chromatography
TOF	turnover frequency
TON	turnover number
TpNb	tetraperoxoniobate
TPNb	triperoxoniobate
V-BPO	vanadium bromoperoxidase
V-HPO	vanadium haloperoxidase
WSP	Water soluble polymer